Autocatalytically Fragmented Light Chain of Botulinum A Neurotoxin Is Enzymatically Active[†,‡]

S. Ashraf Ahmed,[*,#] Peter McPhie,[§] and Leonard A. Smith[#]

Department of Immunology and Molecular Biology, Division of Toxinology and Aerobiology, U. S. Army Medical Research Institute of Infectious Diseases, 1425 Porter Street, Fort Detrick, Maryland 21702, and Laboratory of Biochemistry and Genetics, National Institutes of Diabetes and Digestive and Kidney Diseases, National Institutes of Health, Bethesda, Maryland 20892.

Received March 13, 2003; Revised Manuscript Received July 20, 2003

ABSTRACT: The zinc-endopeptidase light chain of botulinum A neurotoxin undergoes autocatalytic fragmentation that is accelerated by the presence of the metal cofactor, zinc [Ahmed, S. A. et al. (2001) *J. Protein Chem. 20*, 221−231]. We show in this paper that >95% fragmented light chain obtained in the absence of added zinc retained 100% of its original catalytic activity against a SNAP-25-derived synthetic peptide substrate. In the presence of zinc chloride, when >95% of the light chain had undergone autocatalytic fragmentation, the preparation retained 35% of its original catalytic activity. On the other hand, in the presence of glycerol, the light chain did not display autocatalysis and retained 100% of the original activity. These results suggest that the activity loss by incubation with zinc was not a direct consequence of autocatalysis and that the environment of the active site was not affected significantly by the fragmentation. The optimum pH 4.2−4.6 for autocatalysis was different than that (pH 7.3) for intrinsic catalytic activity. Inhibition of autocatalysis at low pH by a competitive inhibitor of catalytic activity rules out the presence of a contaminating protease but suggests a rate-limiting step of low pH-induced conformational change suitable for autocatalysis. Our results of LC concentration dependence of the fragmentation reaction indicate that the autocatalysis occurs by both intramolecular and intermolecular mechanisms.

Seven immunologically distinct botulinum neurotoxins (BoNT),[1] designated BoNT/A-G, are the most potent of all toxins (see refs *2* and *3* for a review). Apart from being potential military threat and bioterrorism agents (*4*), these neurotoxins are also widely used as laboratory research tools (*5*) and as clinical drugs in a variety of neuromuscular disorders of the skeletal, glandular, and smooth muscles and pain disorders, as well as in cosmetic applications (*6*, *7*). These neurotoxins are initially expressed by strains of *Clostridium botulinum* as 150-kDa single polypeptides. Posttranslational cleavage by an endogenous trypsin-like protease generates a 50-kDa N-terminal light chain (LC) and a 100-kDa C-terminal heavy chain (HC) that are still connected by a disulfide bond. The 100-kDa HC can further be proteolyzed into a 50-kDa N-terminal membrane spanning domain (H_n) and a 50-kDa C-terminal receptor-binding domain (H_c). The LC possesses the toxic, zinc endopeptidase catalytic domain, but in the absence of HC, it is nontoxic.

With three functional domains, the mechanism of action of these neurotoxins is multiphasic. The H_c domain plays a role in binding the neurotoxin to specific receptors located exclusively on the peripheral cholinergic nerve endings (*8*). The H_n domain is believed to participate in a receptor-mediated endocytotic pore formation in an acidic environment, allowing translocation of the catalytic LC into the cytosol. Reducing the disulfide bond connecting the LC with the H_n upon exposure to the cytosol or within the acidic endosome (*9*, *10*) is thought to release the catalytic LC into the cytosol. The LC then cleaves at specific sites of one of the three different SNARE proteins, synaptobrevin, syntaxin, or SNAP-25 (*11*−*13*). These proteins are essential for synaptic vesicle fusion in exocytosis. Their proteolysis inhibits exocytosis and blocks acetylcholine secretion, leading ultimately to muscular paralysis and death.

Recombinant LC is catalytically active (*1*) and when injected into sea urchin eggs (*1*, *14*) or injected into mice after reconstitution of the holotoxin by adding HC (*15*), it is

[†] The research described herein was sponsored by the U.S. Army Medical Research and Materiel Command Project No. RIID 02-4-34-064.

[‡] Opinions, interpretations, conclusions, and recommendations are those of the authors and are not necessarily endorsed by the U. S. Army.

* To whom correspondence should be addressed. Tel.: (301) 619−6299. Fax: (301) 619−2348. E-mail: syed.ahmed@amedd.army.mil.

[#] U.S. Army Medical Research Institute of Infectious Diseases.

[§] National Institutes of Health.

[1] Abbreviations: BoNT, botulinum neurotoxin; BoNT/A, botulinum neurotoxin serotype A; LC, light chain; HC, heavy chain; H_n, N-terminal domain of the heavy chain; H_c, C-terminal domain of the heavy chain; SNAP-25, synaptosomal-associated protein of 25 kDa; VAMP, vesicle-associated membrane protein; SNARE, soluble NSF attachment protein receptor; IPTG, isopropyl β-D-thiogalactopyranoside; EDTA, ethylenediamine tetraacetate; TPEN, tetrakis(2- pyridylmethyl)ethylenediamine; SDS−PAGE, sodium dodecyl sulfate polyacrylamide gel electrophoresis; HEPES, *N*-2-hydroxyethylpiperazine-*N*′-2-ethanesulfonic acid; MES, 2-[*N*-morpholino]ethanesulfonic acid; CAPS, 3-[cyclohexylamino]-1-propanesulfonic acid; PVDF, polyvinylidine difluoride; MALDI, matrix assisted laser desorption−ionization; ES-IMS-MS-MS, electrospray ionization mass spectrometry-mass spectrometry; SDS, sodium dodecyl sulfate.

10.1021/bi030062c
Published on Web 10/11/2003

biologically active. DasGupta and Foley (*16*) first observed that BoNT/A and BoNT/E LC prepared in 2 M urea from the whole neurotoxin degrades into two large fragments. Recently, we demonstrated that recombinant BoNT/A LC undergoes C-terminal processing[2] at several sites between residues 419−448 and fragmentation[2] between residues 250 and 267, both by autocatalytic proteolysis (*17*). In that study, which employed a partially zinc-free LC, C-terminal processing was predominant, followed by fragmentation at the F266−G267 bond, and finally a cleavage between Y251−Y252. In the presence of added zinc chloride, fragmentation at Y251−Y252 occurred rapidly, bypassing the cleavage at the F266−G267 bond and followed by C-terminal processing of the C-terminal fragment.

Biological significance of this autocatalysis reaction is not known. Proteolytic modification of proteins by autocatalytic action plays essential roles in making biologically functional, mature products (*18*−*21*). Because the LC is the catalytic moiety of BoNT, with immense military and public health implications and therapeutic applications, detailed characterization of the protein at molecular level is extremely important. Therefore, we followed the consequence of autocatalysis on its catalytic activity on a true substrate mimic. In this paper, we report that autocatalytic fragmentation can occur without significant effects on the intrinsic activity of the LC. We found that in addition to zinc chloride, low pH drastically increases the rate of autocatalysis. By employing active-site inhibitors, we reconfirmed the enzymatic nature of the autocatalysis, and by following LC concentration dependence on the fragmentation, we demonstrated that the autocatalysis occurs by both intramolecular and intermolecular mechanisms.

EXPERIMENTAL PROCEDURES

BoNT/A LC, Chemicals, Buffers, and Reagents. The 448-residue recombinant BoNT/A LC with an extra valine residue at position 2 (*1*) was expressed and purified as described (*17*). The homogeneous preparation was stored at −20 °C in buffer P (50 mM Na-phosphate pH 6.5) containing 150−250 mM NaCl and 2 mM EDTA. The protein was desalted by passing through a PD-10 gel filtration column and was collected in appropriate buffer before each experiment and assays. Buffer P (50 mM Na-phosphate pH 6.5) was used throughout except in the enzyme assays where 50 mM Na-HEPES pH 7.4 was employed. Zinc chloride was obtained from Sigma. Rabbit polyclonal antibodies against a 16-residue N-terminal sequence (PFVNKQFNYKDPVNGV) of BoNT/A LC were produced and affinity-purified by Research Genetics (Huntsville, AL). Affinity-purified, peroxidase-coupled goat anti-rabbit and anti-mouse IgG (H + L) and ABTS substrate were from Kirkegaard Perry Laboratories (Gaithersburg, MD). The peptide inhibitor I (Ac-CRATKML-NH_2) (*22*) was synthesized and purified by Cell Essentials (Boston, MA). The peptide inhibitor II (2-mercapto-3-phenylpropionyl-CRATKML-amide) (*23*) was a generous gift from Dr. J. J. Schmidt.

[2] "C-terminal processing" and "truncation" are interchangeably used in this paper to denote either sequential or random removal of 4−28 residues from the C-terminus of the LC. "Fragmentation" denotes cleavage of the LC or the truncated LC into two large fragments with mass > 15 kDa.

Autocatalysis Experiments. Before each experiment, aliquots of the LC were thawed to room temperature and immediately passed through a PD-10 gel-filtration column equilibrated with buffer P. The protein was collected in buffer P and stored on ice. The LC was mixed with predetermined concentrations of $ZnCl_2$ or glycerol, and 5 μL (for activity assays) and 50 μL (for SDS−PAGE) aliquots were distributed in screw-capped Eppendorf tubes. The final concentration of the protein was 0.17 mg/mL (3.3 μM) in these incubation mixtures. The tubes were incubated at 22 °C. At various time intervals, 25 μL of 2× SDS-load buffer was added to a 50 μL aliquot for SDS−PAGE analysis. At the same time intervals, the 5 μL aliquots were used for catalytic activity assays (see later).

SDS−PAGE and Western Blot. SDS−PAGE was carried out under reducing conditions (*24*) on 1-mm-thick 10% tricine-gels (Novex) as described (*25*). Samples were boiled for 5 min in 0.4% SDS, 5% β-mercaptoethanol, 12% glycerol, and 450 mM tris-HCl (pH 8.45) by boiling for 5 min. The running buffer contained 0.1% SDS in 0.1 M tris-0.1M tricine, pH 8.3. The gels were stained with Coomassie Brilliant Blue. Protein bands were scanned in a BioRad GS-710 densitometer gel scanner with Quantity One software, and the relative amount of proteins in stained bands in each lane were quantified. Identity of LC and its N-terminal fragments were confirmed by Western blots on nitrocellulose membranes that were prepared by using a primary polyclonal antibody against a 16-residue N-terminal sequence of BoNT/A LC and a peroxidase-coupled goat anti-rabbit IgG (H+L) as the secondary antibody (*1*).

Enzymatic Activity Assays. The enzymatic assay was based on HPLC separation and measurement of the cleaved products from a 17-residue C-terminal peptide corresponding to residue 187−203 of SNAP-25 (*1*, *26*). A master reaction mixture lacking the LC was made and aliquots were stored at −20 °C. At the time of assay, an aliquot of the master mix was thawed and 25 μL was added to 5 μL of the LC (see above) to initiate the enzymatic reaction. Components and final concentration in this 30-μL reaction mixture were 0.9 mM substrate peptide, 0.25 mM $ZnCl_2$, and 0.16−0.55 nM LC, 0.5 mg/mL bovine serum albumin (BSA), and 50 mM Na-HEPES, pH 7.4. BSA was included because in some experiments, it gave higher activity (unpublished). $ZnCl_2$ was included in the assay mixture despite its inhibitory effect (see Results) to make the assay conditions similar, as one LC incubation contained $ZnCl_2$ before the assays. After a 3−5 min incubation at 37 °C, the reaction was stopped by acidifying with 90 μL of 0.7% TFA, and 100 μL of this mixture was analyzed by HPLC as described (*1*). For K_m and V_{max} determinations (Figure 2C), the reaction mixtures were incubated at 23 °C.

UV−Visible Absorption, Circular Dichroism and Fluorescence Measurements. To determine protein concentration and to assess purity, UV−visible absorption spectra were recorded at 22 °C with a Hewlett-Packard 8452 diode array spectrophotometer. LC concentration was determined using $A^{0.1\%}$ (1-cm light path) value of 1.0 at 278 nm (*17*) or by BCA assay (Pierce) with BSA as standard. Both methods give the same result.

Circular dichroism spectra were recorded at 20 °C (10 °C for Zn-autocatalyzed LC), with a Jasco 718 spectropolarimeter with quartz cuvettes of 1-mm path length. An average

of five scans were recorded to increase signal-to-noise ratio at a scan speed of 20 nm/min with a response time of 8 s. In all measurements, a buffer blank was recorded separately and subtracted from sample recordings. Mean residue weight (114.55) was calculated by using a molecular mass of 51 318.4 Da for the 448-residue LC (*17*). Secondary structural contents were calculated by SELCON supplied in the Softsec program (Softwood, Co.).

Tryptophan fluorescence emission spectra were recorded at 20 °C (10 °C for Zn-autocatalyzed LC) in a PTI QuantaMaster spectrofluorimeter, model RTC 2000 equipped with a Peltier controlled thermostat and Felix software package. Emission and excitation slit widths were set at 1 nm and excitation wavelength at 295 nm. Each spectrum was an average of five scans.

RESULTS

The BoNT/A LC Preparation. The recombinant LC used in this report was expressed in *Escherichia coli* and purified as described (*17*), and was judged near homogeneous from Coomasie stained SDS−PAGE gels (Figure 1). A specific activity of 3.2 μmol min^{-1} mg^{-1} of this preparation in the absence of added zinc against a 17-mer SNAP-25 peptide substrate was obtained. Adding 0.25 mM $ZnCl_2$ to the assay mixture decreased the specific activity to 2.4 μmol min^{-1} mg^{-1}. Adding BSA to the reaction mixture stimulated the activity but did not affect the inhibitory action of zinc. Thus, when assayed in the presence of 0.5 mg/mL BSA and 0.25 mM $ZnCl_2$, the specific activity was increased to 3.72 (Figure 2B). We did not explore the BSA effect further but included it in some reaction mixtures to conveniently calculate low levels of activity.

Autocatalysis and Catalysis of BoNT/A LC. We define autocatalysis as the process that results in autolysis of the LC into fragments by one or more cleavage, and catalysis as the cleavage of a soluble, SNAP-25 peptide substrate catalyzed by the LC. We reported earlier that BoNT/A LC underwent autocatalytic degradation when stored at 4 °C (*17*). To investigate any consequence of this autocatalytic degradation on the intrinsic catalytic activity, we incubated LC in 50 mM Na-phosphate buffer (pH 6.5) at room temperature (22 °C). At various time intervals, an aliquot was analyzed by SDS−PAGE for structural integrity of the LC (Figure 1). In the absence of exogenous zinc, the LC remained intact for 164 h, but thereafter it was degraded first into IB (V1−Y426)[3] and then into fragments designated as IIIB (V1−Y251), IVB (Y252−F423), and IVC (G267−F423) (Figure 1A). In the presence of $ZnCl_2$, the LC rapidly degraded into two major fragments, IIIB and IVA (Y252−K448) (Figure 1B), and unlike in Figure 1A, no IB was detected. Peptide designations and identity of fragments were based on their locations on SDS−PAGE (Figure 1) and Western blots (not shown) as they were previously identified by N-terminal sequence, ESI-MS, and ESIMS-MS determinations (*17*). In the presence of glycerol, the LC remained mostly intact

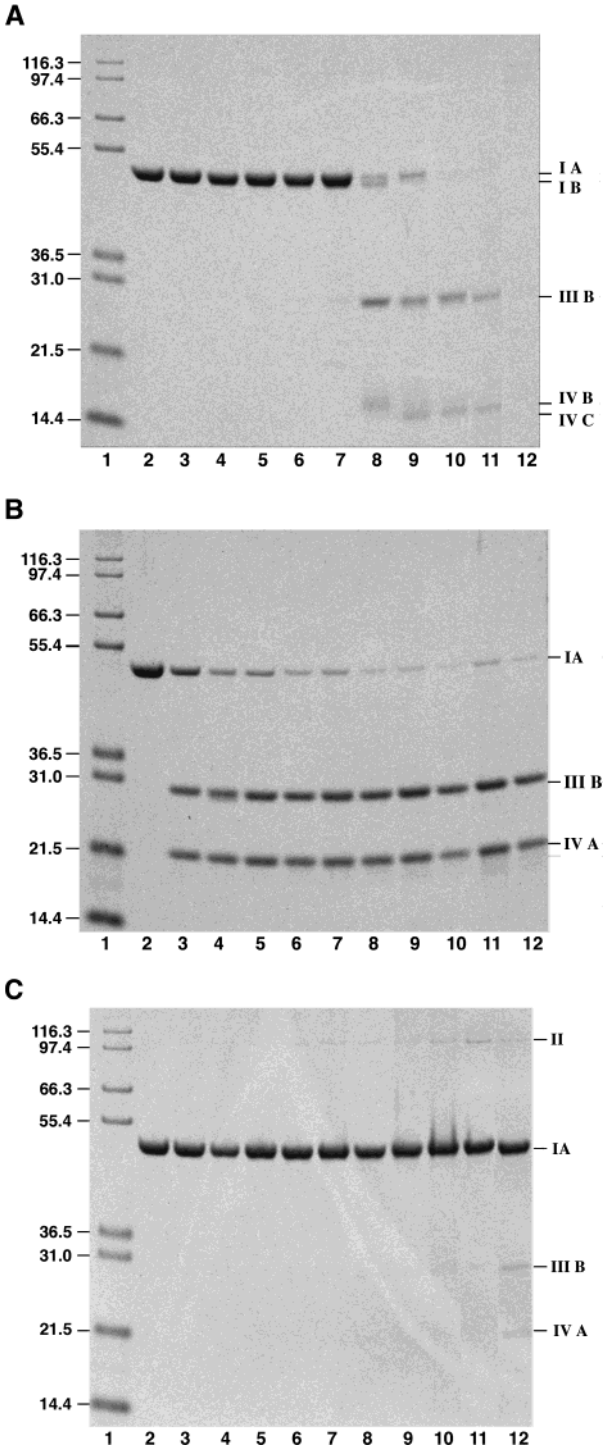

FIGURE 1: Time course of autocatalytic proteolysis of BoNT/A LC at pH 6.5 in the absence (A) and presence of 0.5 mM $ZnCl_2$ (B) or 10% glycerol (C). 100 μL aliquots (0.17 mg/mL of buffer P) of the LC were incubated at room temperature (22 °C). At intervals 0.05 mL of 2× SDS-load buffer was added to an aliquot and boiled for 5 min. Lane 1 shows Novex Mark-12 molecular mass markers with indicated molecular masses. Lane 2−12 represents 0, 20, 44, 72, 116, 164, 212, 235, 259, 311, and 362 h of incubation. Peptide designations[3] at right are from ref *17*: IA, full-length LC with residues V1−K448; IB, LC residues V1−Y426; II, a dimer of IA and/or IB; IIIB, LC residues V1−Y251; IVA, residues Y252−K448; IVB, Y252−F423; IVC, G267−F423. Variations in the amount of sample application partly account for the differences in the intensity of bands in some adjacent lanes. The extent of autocatalysis was therefore calculated in terms of percent of LC remaining intact as IA in each lane and data were plotted in Figure 2A.

[3] Peptide designation uses sequences of the recombinant LC that contain one extra valine after the initial methionine, and as reported in Table 2 of ref *1*. Their identity in the two schemes in that report does not take account of the extra valine of the recombinant LC. Fragment IB having a sequence stretch of V1−Y426 is also defined as V1−F423 as was explained at the legend of Scheme 1 (ref *1*).

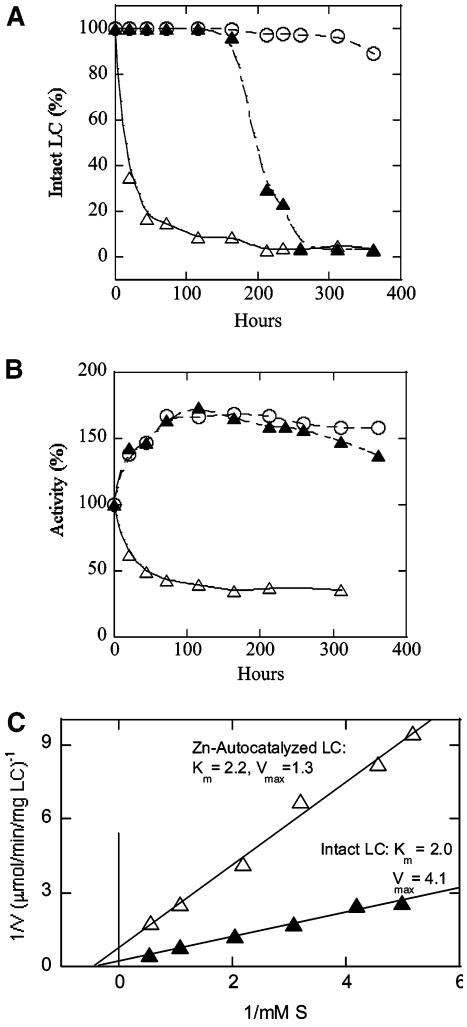

FIGURE 2: Comparison of autocatalysis (A) with catalysis (B) of BoNT/A LC as a function of incubation time at pH 6.5 and room temperature (22 °C). (A) The Coomassie blue-stained SDS gels in Figure 1 were scanned densitometrically and the results, expressed as percent of the LC remaining intact in each lane, are plotted. (B) Five microliter aliquots of the LC in screw-capped Eppendorf tubes were incubated under the conditions of Figure 1. Intrinsic catalytic activity on these aliquots was determined with a synthetic, SNAP-25-derived substrate (see Experimental Procedures) at pH 7.4 in triplicate for each data point. 100% activity in the absence of any additive represents a specific activity (SA) of 3.72 μmol min^{-1} mg^{-1} LC; in the presence of $ZnCl_2$, 2.69 μmol min^{-1} mg^{-1} and in the presence of glycerol, 4.04 μmol min^{-1} mg^{-1}. Incubating LC at room temperature (22 °C) was in the absence (closed triangle) or presence of 0.5 mM $ZnCl_2$ (open triangle) or 10% glycerol (open circle). (C) Double reciprocal plot of substrate concentration versus reaction velocity for catalytic cleavage of the synthetic, SNAP-25-derived substrate by intact (closed triangle) and zinc-autocatalyzed LC (open triangle). Each data point represents an average of 4−5 determinations. Autocatalyzed LC was prepared by 168 h of incubation of intact LC with 0.5 mM $ZnCl_2$ as described in Figure 5 legend. LC preparation used in this experiment and Figure 5 was different than used in rest of the paper in that it was frozen at −20 °C for more than two years.

during the incubation (Figure 1C). Glycerol appeared to protect the structure of the LC. In the presence of glycerol, however, a dimeric species, II, in the pathway of autocatalysis (*17*) was clearly detectable. One notable feature is that the incubation mixtures both in the presence or absence of $ZnCl_2$, showed the presence of 3% of intact LC even after prolonged incubation (Figure 2A). We have no explanation, but this residual intact LC may represent a precipitated LC formed during incubation that may have escaped fragmentation.

To determine the catalytic activity of the autocatalytically fragmented LC, we determined the extent of LC remaining intact upon incubation as shown in Figure 1 and plotted the results in Figure 2A. Figure 2B shows the catalytic activity of the LC as a function of incubation time under identical conditions of Figure 1. In the absence of any additive or in the presence of glycerol, the catalytic activity of the LC increased about 1.7-fold after incubation at 22 °C for 116 h. Upon further incubation the activity slowly decreased, yet the lowest activity measured (137%) was 37% higher than the original. In contrast, in the presence of $ZnCl_2$, catalytic activity of the LC at first rapidly decreased, but after 100 h, 35−40% of the activity was retained (Figure 2A) although most (>96%) of the LC was degraded (Figure 2A). Although in the presence of glycerol, most of the LC remained intact and active (Figures 2A and 1C), in the absence of any additive, most of the LC (>96%) was degraded (Figures 2B and 1A), yet most of the catalytic activity was retained. Glycerol thus appeared to protect both the structure and activity of the LC. Comparison of the results of Figure 2A,B demonstrated that autocatalytically fragmented LC retained its intrinsic catalytic activity.

We also determined the substrate affinity, K_m, of autocatalyzed LC for the synthetic 17-residue SNAP-25 peptide substrate. Figure 2C shows that K_m, 2.2 mM, of a Zn-autocatalyzed LC did not change appreciably from that of the intact LC, 2.0 mM. The corresponding V_{max}, 1.3 μmol min^{-1} mg^{-1} LC at 23 °C, is 30% of the intact LC V_{max} of 4.1 μmol min^{-1} mg^{-1}, similar to the specific activity difference observed in Figure 2B above.

Effects of pH on Catalysis and Autocatalysis. We determined the optimum pH of the LC for autocatalysis and catalysis employing four buffers with an overlapping pH range of 3−9 (Figure 3A,B). Because autocatalysis must occur at the active site, one can expect the pH optima for autocatalysis and catalysis to be same. On the contrary, we found that while the optimum pH for catalysis was 7.2−7.4 (Figure 3B), that for autocatalysis was 4.6 (Figure 3A). Using a narrow pH increment of 0.2 of the acetate buffer and a shorter incubation time of 5 h, we found the optimum pH was 4.2−4.6 (not shown). The experiments in Figure 3A were carried out in the presence of $ZnCl_2$ in which the fragmentation pattern as shown in Figure 1B were observed at all pH. In experiments without $ZnCl_2$ and with much longer incubation time (not shown), the fragmentation pattern at low pH was similar to that observed in the presence of $ZnCl_2$ as shown in Figure 1B in that fragment IVA was produced, but at higher pH the pattern was similar (not shown) to those observed in Figure 1A. Quantitative analysis and plots of percent LC remaining intact against pH (not shown) nonetheless yielded a pH−activity curve similar to that shown in Figure 3A and an identical optimum pH of 4.6.

Active-Site Inhibitors of BoNT/A LC Inhibit Autocatalysis. Earlier, we showed that TPEN, a metal chelator, and CTKRML (peptide inhibitor I, K_i, ~2 μM) (*22*), a competitive inhibitor of BoNT/A LC inhibited fragmentation of the LC (*17*). To further eliminate the possibility of a contaminating protease in our LC preparation, we used another inhibitor (peptide inhibitor-II) having a K_i of 0.3 μM (*23*) in addition

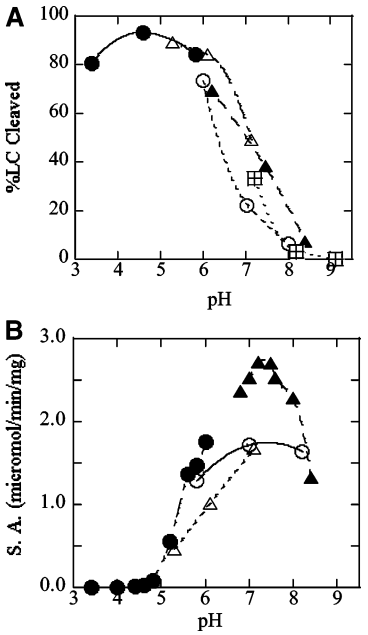

FIGURE 3: Effects of pH on autocatalysis (A) and catalysis (B). (A) A stock solution of LC (in 10 mM Na-phosphate buffer pH 6.5) was diluted more than 4-fold to a final concentration of 0.17 mg/mL with 50 mM solutions of the indicated buffers and incubated with 0.5 mM $ZnCl_2$ for 17 h at room temperature (22 °C). Coomassie blue-stained SDS−PAGE gels were developed as described in the legends of Figure 1 and densitometrically scanned as described in the legend of Figure 2A. (B) Intrinsic catalytic activity of LC (0.014 mg/mL) in various buffers (38 mM) was assayed in duplicate at 37 °C. Buffers: acetate (closed circle), MES (open triangle), HEPES (closed triangle), Na-phosphate (open circles), and tris-HCl (square).

to the peptide inhibitor-I used previously. We first incubated the LC separately with the two inhibitors at pH 6.5 for 10 min. One reaction mixture was then acidified to pH 4.7 and the incubation was continued for 17−72 h. Figure 4A shows that at pH 4.7, fragmentation was less (than control) in the presence of peptide I, but this peptide was not very effective in preventing the LC from fragmentation. However, peptide II was more effective than peptide I and greatly reduced the fragmentation so that 30% of the LC was intact compared to only <5% in the control experiment. At pH 6.5 (Figure 4B), both peptides completely prevented the fragmentation. Both inhibitors are competitive with substrate (*22*, *23*). Therefore, failure of either inhibitor to completely inhibit the fragmentation at low pH is most probably due to dissociation of the inhibitors from the active site at low pH.

As a more direct proof that autocatalysis is not due to a contaminating protease, we employed three mutant LCs. Conservative replacement of residues Y366 and R363 severely impaired catalysis, and these residues were implicated in transition state stabilization (*27*). When incubated with 0.5 mM $ZnCl_2$ for 20 h, the LC mutants Y366F and R363L remained fully intact, while 70% of the wild type LC underwent fragmentation. Thermostability and spectroscopic properties of these poorly active (0.1−2% of wild type) proteins showed that their structures did not significantly differ from that of the wild-type LC. As a negative control, a naïve mutant E63A with full catalytic activity was degraded to 68% under similar conditions.

Dependence of LC Concentration on Autocatalysis. To distinguish between intermolecular and intramolecular reactions, we determined the rates of autocatalysis as a function of LC concentration at two pH values of 6.5 and 5.0 (Figure 5). At all concentrations of LC, the rate of autocatalysis in acetate buffer pH 5.0 (Figure 5B) was 40-fold faster than in phosphate buffer pH 6.5 containing $ZnCl_2$ (Figure 5A), and followed first-order kinetics, as shown for a LC concentration of 0.2 mg/mL. At this concentration, half-life of the light chain was 15.1 ± 0.8 min at pH 5.0 and 11.75 ± 0.93 h at pH 6.5 containing $ZnCl_2$. The rates of reactions, and the rate constants increased with concentration of LC in the range of 0.05−1.8 mg/mL (Figure 5A), indicating it to be an intermolecular (or bimolecular) reaction. At either pH, the extrapolated rate constant, *k*, to zero LC concentration, however, is far from zero, indicating it to be a unimolecular or intramolecular reaction at low LC concentration. Half-life at pH 5.0 was calculated as 17 min at zero protein concentration.

Structural Features of LC at Low pH and in the Presence of Zinc. To detect and identify any conformational changes induced by zinc or low pH, we collected far-UV circular dichroism and tryptophan fluorescence spectra of the LC at pH 6.5 with and without 0.5 mM $ZnCl_2$ and at pH 4.67 (no added zinc). The CD spectra that measures secondary structure of proteins were very similar in the three conditions (Figure 6A). The CD results calculated as % secondary structure are summarized in Table 1. The structural content of intact and fragmented LC at pH 6.5 is not significantly different, but there appears to be a general increase in the helical content of the intact LC in the presence of $ZnCl_2$ or at low pH. Like the small difference in the secondary structural contents, both zinc and low pH appear to little affect the tryptophan fluorescence spectra (Figure 6B) and yield of the LC (Table 1), with $ZnCl_2$ affecting more than low pH. The blue-shifted tryptophan fluorescence emission spectra with a λ_{max} of 324 nm (λ_{max} of free tryptophan is about 354 nm) are similar to those observed by Li and Singh (*28*) and suggest that the two tryptophan residues are buried in a hydrophobic environment that is not affected by either low pH or zinc.

CD and tryptophan fluorescence spectra of a fragmented LC prepared by incubation with $ZnCl_2$ (not shown) showed very little difference with the intact LC in the former, but the fluorescence intensity decreased by 26% (Table 1) without affecting the emission maximum or shape of the spectrum (not shown). The results of the CD and fluorescence experiments suggest that although the secondary structure of the fragmented LC is not significantly different than that of the intact LC, there may be some conformational or tertiary structural changes in the fragmented LC.

Thermal Denaturation of Intact and Autocatalytically Fragmented LC. Temperature-dependent unfolding of LC was followed by monitoring CD at 222 nm (Figure 7). In contrast to lesser differences in the secondary structural contents (Figure 6A, Table 1), the unfolding pattern of LC determined under three different conditions differed significantly. We could not determine the thermodynamic parameters because the thermal denaturation was irreversible. The thermal denaturation curves shown in Figure 7 nonetheless allowed calculation of the apparent melting temperature, T_m (midpoint of thermal transition) values (Table 1). A sharp, monophasic denaturation curve was obtained at pH 6.5 in the absence of $ZnCl_2$ (Figure 7), indicating that the LC

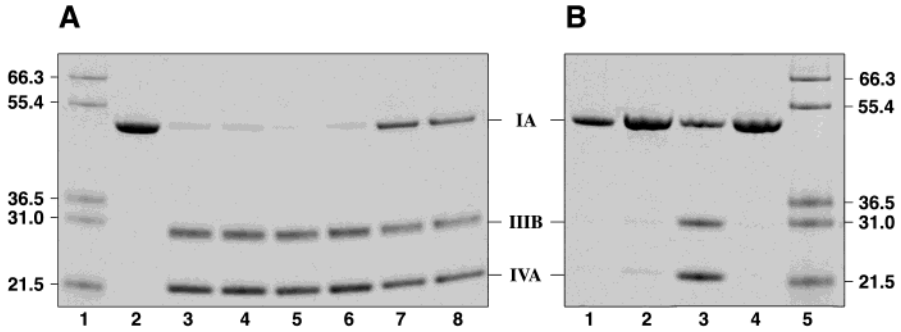

FIGURE 4: Inhibition of autocatalysis by active-site inhibitors at pH 4.67 (A) and at pH 6.5 containing 0.5 mM $ZnCl_2$ (B) as shown by SDS−PAGE. The LC (0.2 mg/mL) was incubated without or with 1.4 mM peptide inhibitor I, or 2 mM peptide inhibitor II in 43 mM Na-acetate pH 4.67 or 50 mM Na-phosphate pH 6.5 plus 0.5 mM $ZnCl_2$, all containing 4 mM DTT. The pH 4.67 incubation (A) was for 20 h and the pH 6.5 plus $ZnCl_2$ incubation (B) was for 72 h, both at 22 °C. Lane 2 (lane 1 in panel B) represents intact LC; lanes 3−4 (lane 2 in B), LC + peptide inhibitor I; lanes 5−6 (lane 3 in B), LC + none; lanes 7−8 (lane 4 in B), LC + peptide inhibitor II; and lane 1 (lane 5 in B), molecular mass markers.

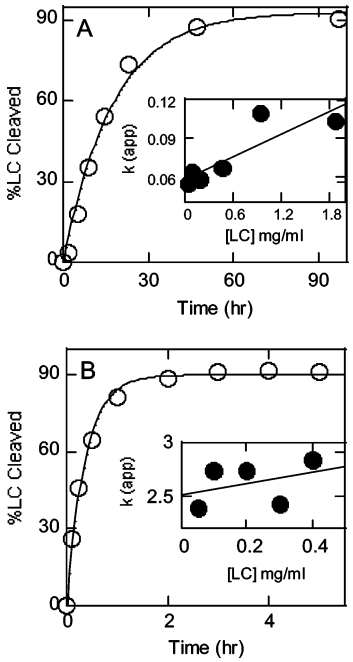

FIGURE 5: Dependence of autocatalytic rates on LC concentration. Progress curves of autocatalysis at pH 6.5 containing 0.5 mM zinc chloride (A) and at pH 5.0 without zinc chloride (B) at a LC concentration of 0.2 mg/mL, 23 °C. The rate constants, *k*, were calculated by first-order fits [% cleaved = maximum cleaved × (1 − e^{-kt})] of the data points at various LC concentrations and are shown in the inset. LC (1.8 mg/mL, 50 mM Na-phosphate, pH 6.5) was diluted to indicated concentrations, and autocatalysis was followed by SDS−PAGE and densitometric scans of stained gels as described in Experimental Procedures. For pH 5.0 data, LC (1.41 mg/mL, 10 mM Na-phosphate, pH 6.5) was diluted to indicated concentrations with 100 mM Na-acetate pH 5.0. The choice of higher concentration of acetate was to ensure a stable pH after dilution. Aliquots were removed to stop the reaction with SDS load buffer, and the extent of autocatalysis was followed.

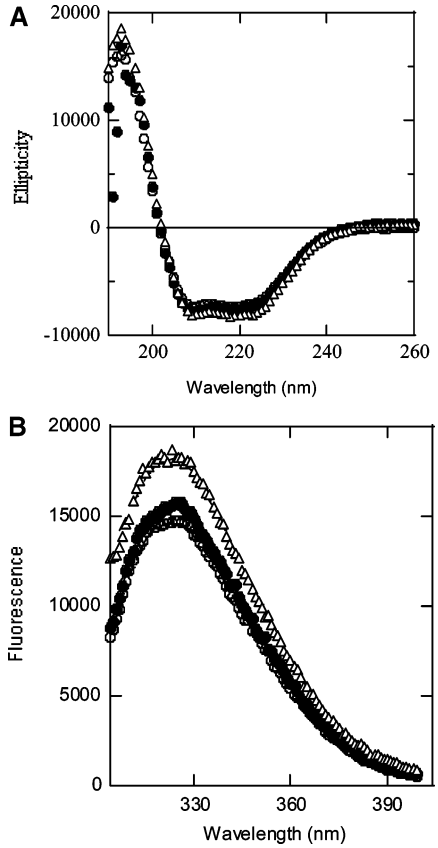

FIGURE 6: Far UV circular dichroism (A) and tryptophan fluorescence emission (B) spectra of LC at 6.5 (open circle), at pH 4.7 in 43 mM Na-acetate (closed circle), and at pH 6.5 in the presence of 0.5 mM $ZnCl_2$ (triangle) in buffer P.

preparation was homogeneous, and yielding a T_m of 41.5 °C. The denaturation curve at pH 6.5 in the presence of $ZnCl_2$ appeared to be biphasic with an inflection point at about 58 °C, and yielded a higher T_m of 54 °C. At pH 4.7, increasing the temperature increased the ellipticity at 222 nm (Figure 7) as was observed by others (*28*), and a T_m of 50 °C was calculated for this thermal transition. Thus, both low pH and presence of $ZnCl_2$ at higher pH significantly stabilized the LC as indicated by an increase in T_m by 9−12 °C. The T_m of the autocatalytically fragmented LC, determined in the presence of $ZnCl_2$, was between those of the intact LC at pH 6.5 in the presence and absence of $ZnCl_2$ (Table 1). Although fragmented LC appeared to be more stable than intact LC, this might have been due to the effect of $ZnCl_2$.

DISCUSSION

We demonstrated recently that the LC undergoes autocatalytic fragmentations at the Y250−Y251 and F266−G267 bonds (*17*). By following the kinetics of this autocatalytic reaction in parallel with measurement of intrinsic catalytic activity toward the soluble SNAP-25 peptide substrate, we conclusively demonstrated in this report that autocatalysis does not have any direct consequence on the intrinsic activity

Table 1: Calculated Secondary Structural Content, Tryptophan Fluorescence,[a] and Melting Temperature of Intact and Autocatalytically Fragmented LC under Various Conditions

LC	pH	addition	% α-helix	% β-sheet	% turns	% random coil	Trp Fluo (Rel)	T_m (°C)
intact	6.5	none	27.5	20.8	17.7	30.5	1.0	41.5
	6.5	$ZnCl_2$	28.6	21.6	15.6	29.6	1.23	54.0
	4.7	none	36.6	19.4	19.4	25.0	1.06	50.0
	8.1[b]	NaCl	22.0	27.5	18.75			
fragmented	6.5	$ZnCl_2$	28.2	18.0	17.6	32.3	0.77	47.0

[a] CD and Trp fluorescence spectra were collected at 20 °C except for the fragmented LC at pH 6.5, collected at 10 °C. At the lower temperature, ellipticity at 220 nm and fluorescence emission slightly increases, and were ignored. [b] LC separated from purified BoNT/A, data from ref *51*.

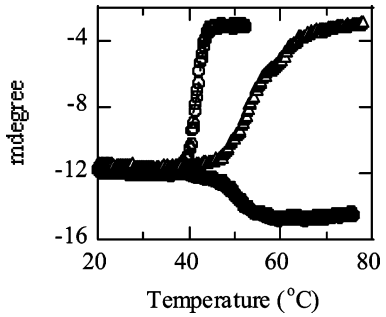

FIGURE 7: Thermal unfolding of LC at 6.5 (open circle), at pH 4.7 in 43 mM Na-acetate (closed circle), and at pH 6.5 in the presence of 0.5 mM $ZnCl_2$ (triangle) in buffer P as monitored by circular dichroism at 222 nm. Protein concentration in these experiments was 0.17−0.2 mg/mL. The midpoint of thermal transition, T_m, calculated from this experiment and others not shown are summarized in Table 1.

of the BoNT/A LC. Several lines of evidence led us to this conclusion: (a) No significant degradation was observed during the first 116 h of incubation in the absence of any additive (Figures 1A and 2A), although the intrinsic catalytic activity increased by 70% during this period (Figure 2B). (b) Although degradation of LC was observed after 164 h, eventually resulting in >96% degradation (Figure 2A), there was only a small decrease (<20% from the highest value) in activity during this period (Figure 2B). (c) A rapid degradation accompanied the incubation with $ZnCl_2$, resulting in >90% degradation during the first 116 h (Figure 2A); nonetheless, 40% of the intrinsic activity was retained. The lowered activity was partly due to greater inhibition of activity of the fragmented LC by higher concentration of exogenous zinc, as observed earlier with a LC purified from inclusion bodies (*1*) and other zinc proteases (*29*). As the autocatalyzed LC was prepared in the presence of 0.5 mM $ZnCl_2$, the assay mixture for its catalytic activity (see Experimental Procedures) contained 0.33 mM $ZnCl_2$ as opposed to 0.25 mM $ZnCl_2$ in all other catalytic activity assay mixtures. An additional possibility for this lowered activity may have been due to more favorable interaction of zinc with the fragment IVA (Figure 1B) produced in the presence of $ZnCl_2$ that was larger than IVB and IVC (Figure 1A) produced in the absence of $ZnCl_2$. (d) Adding glycerol almost completely protected the LC from degradation, yet the same initial increase in catalytic activity was observed as in the absence of any additive. Stabilization of proteins by polyols such as glycerol is well-known and is possibly the result of enhanced protein folding (*30*). We have not further investigated the increase in catalytic activity during storage either in the absence or presence of glycerol.

Enzymatic Nature of the Autocatalytic Reaction. In the earlier report (*17*), we characterized the autocatalytic reaction of LC by mapping the autocatalytic sites. We also provided evidence that the reaction is significantly inhibited by the metal chelator, TPEN, and a competitive peptide inhibitor of BoNT/A catalytic activity. These results led us to conclude that the autocatalytic reaction was enzymatic in nature and occurs at the same active site of its endopeptidase activity. However, the apparent slow fragmentation reaction occurring over hours and days of incubation at room temperature (22 °C) (Figures 1, 2A, and 3A) compared to minutes of incubation for the catalytic reaction on a peptide substrate at 37 °C (Figures 2B and 3B) may mislead one to wonder if the former is nonenzymatic. Three considerations suggest that the autocatalysis reaction rate should be higher than reported here. (a) If the autocatalysis reactions were followed at 37 °C, it would be expected to increase by 3−5-fold. We avoided incubation at higher temperature because of relatively low thermostability of LC (Figure 7 and Table 1) in phosphate buffer in which the autocatalysis experiments were conducted. (b) In the autocatalytic reaction, the substrate is the enzyme itself. From the first-order kinetics observed in Figure 5, we conclude that the $K_m \gg 35$ μM (1.8 mg/mL). Thus, the reaction rate is greatly limited by LC concentration. (c) The autocatalysis reaction was limited by a putative, low pH-induced conformational change of LC (see later). Hence, at pH 6.5 (Figure 2A) only a marginal fraction of LC will be available as a substrate. Therefore, the extent of autocatalysis around neutral pH was limited by substrate availability. Moreover, LC concentrations employed (<0.6 nM) in the enzymatic assays (Figure 2B) were considerably lower than employed (3.3 μM) in autocatalysis (Figure 2A) to capture "initial" rates in the former case and to detect low levels of fragmentation by Coomassie staining (see Experimental Procedures) in the latter. Recent biophysical studies with BoNT/A established that the neurotoxin is 4-fold more active as a monomer at <50 nM concentration than as a dimer at a higher concentration (*31*). If a similar concentration dependence of monomer−dimer equilibria holds for LC, it may partly account for the low autocatalytic activity. Apart from these considerations, a side-reaction catalyzed by an enzyme can be very slow. For example, a tryptophan cleavage reaction is 4 orders of magnitude slower than tryptophan synthetic reaction catalyzed by bacterial tryptophan synthase (*32*).

The most unambiguous proof that the autocatalysis reaction is enzymatic in nature comes from use of peptide inhibitors (Figure 4A,B) and mutant LC (not shown). A high-affinity competitive inhibitor of BoNT/A LC activity more efficiently inhibited the reaction than a low-affinity competitive inhibitor at pH 4.7 (Figure 4A), and both almost completely protected LC from degradation at pH 6.5 (Figure 4B). Because these competitive inhibitors must bind at the

active site of LC, inhibition of degradation must also be occurring at the active site. Finally, two mutant LCs with impaired catalytic activity, showed no sign of autocatalytic degradation (see Results). Therefore, autocatalysis and catalysis must be catalyzed at the same enzyme active site making the former enzymatic in nature. These results also provide convincing evidence that the degradation of LC was not due to a contaminating protease.

Effects of Low pH and Zinc Are Similar on Autocatalysis. In qualitative and in rate comparisons, the autocatalytic fragmentation appeared to be similarly affected by low pH and zinc. Autocatalysis of LC in the presence of $ZnCl_2$ generated fragments IIIB and IVA as shown in Figure 1B, and this pattern was consistent at all pH values. In the absence of zinc, two fragmentation patterns were observed: (a) at low pH the pattern was identical to that observed in the presence of zinc as shown in Figure 1B, and (b) at high pH of 7−9 the pattern was as expected in the absence of zinc as shown in Figure 1A. $ZnCl_2$ and low pH thus qualitatively produced the same autocatalysis at Y251−Y252 bond. We also found that the extent of autocatalysis was dramatically enhanced by both $ZnCl_2$ and low pH: most of LC was rapidly degraded at pH 4.7 in the absence of zinc (Figure 4A), as at pH 6.5 in the presence of zinc (Figure 4B). In addition to these observations, enhanced thermostability of LC induced by low pH and zinc also support that these two agents had the same or similar role on the autocatalysis.

Kinetic analysis of concentration dependence of autocatalysis data at low pH 5.0 and at pH 6.5 in the presence of $ZnCl_2$ indicates that the autocatalysis is both intramolecular and intermolecular (Figure 5). The situation appears complex, and a more thorough kinetic study is needed to get a clearer picture. However, an analogy with pepsin−pepsinogen autocatalysis model (*33*) offers a reasonable explanation of our data. The time courses of the intramolecular (eq 1) and intermolecular (eq 2) reactions, having two distinct rate

$$A \xrightarrow{k_1} B \tag{1}$$

$$A + B \xrightarrow{k_2} 2B \tag{2}$$

constants of k_1 and k_2, respectively, were analyzed by McPhie (*33*) to show that if the initial concentration of protein is A_o, and A is concentration of the starting protein species at any time, t, then,

$$\log \frac{k_1 A}{[A_o(k_1 + k_2 A_o) - k_2 A]} = -(k_1 + k_2 A_o)t \tag{3}$$

Initially, the reaction follows pseudo-first-order (intramolecular) kinetics (eq 4):

$$A = A_o e^{-kt} \tag{4}$$

where the apparent rate constant, $k = (k_1 + k_2 A_o)$, but at later times, depending on the relative values of k_1 and $k_2 A_o$, the intermolecular reaction (eq 2) will predominate.

The sigmoidal curve of (control) fragmentation reaction at pH 6.5 in the absence of $ZnCl_2$ with an extended lag time (Figure 2A, closed triangle) is characteristic of an intermolecular autocatalytic reaction (eq 2), which must await accumulation of sufficient species B by the slow intramolecular reaction (eq 1). These data of Figure 2A were analyzed with eq 3 (*33*) to estimate the values of k_1 as 2.1×10^{-5}/h, and k_2 as 0.23/mg/h. Least-squares analysis of the concentration dependence of the autocatalytic rates (Figure 5) yielded k_1 and k_2 values of 0.06/h and 0.7/mg/h at pH 6.5 containing $ZnCl_2$, and 2.4/h and 0.5/mg/h at pH 5.0, respectively. Although k_1 is 40 times higher at pH 5.0 than at pH 6.5 containing $ZnCl_2$, it is much higher under these conditions than at pH 6.5 in the absence of $ZnCl_2$. Thus, lowering of pH to 5.0 or inclusion of $ZnCl_2$ at pH 6.5 stimulated the intramolecular phase of the autocatalytic reaction by more than 10^3−10^5-fold, while rate of the intermolecular reaction is increased only 2−3-fold. A simple acid catalysis of the intramolecular reaction is unlikely since a drop of 1.5 pH units will be expected to a maximum 30-fold stimulation.

Although a Y251−Y252-cleaved dimeric structure have been known (*34*), the structure of LC (of BoNT/A) at the currently available 3.3 Å resolution (*35*) does not offer a structural interpretation of the possible intramolecular step.

The optimum pH for autocatalysis is almost 3 pH units lower than the optimum pH for intrinsic catalytic activity (Figure 3). The simplest explanation for the low pH optima for autocatalysis is that a low pH induces a conformational change in the molecule such that the cleavable bonds are optimally poised at the active site of the same or another molecule for cleavage. It is possible that exogenous zinc also induced a similar conformational change. The data shown in Figure 7 indicate that the conformation of LC is stabilized by addition of zinc or by lowering the pH. In the case of the metal ion, this may be achieved by specific binding of the metal to the native form of the protein. At low pH, acidic groups may be titrated, reducing disruptive electrostatic interactions in the native form. These changes in conditions have very large effects on the rate (k_1) of self-cleavage of LC (see above and Figures 3 and 5), which are most readily explained by an ensuing conformational change in the molecule, into a more easily cleavable state. However, invariance of the CD and fluorescence spectra of LC as shown in Figure 6, indicates that this putative conformational change does not involve large changes in secondary and tertiary structures. In this study, we employed 50 mM Na-phosphate pH 6.5, and 43 mM Na-acetate (plus 7 mM Na-phosphate) pH 4.7. Using 50 mM K-phosphate (containing 100 mM KCl, 1 mM β-mercaptoethanol, and 0.05% dodecylphosphocholine) pH 7.0, 5.0, and 4.5, other investigators, however, reported a (hyperbolic) decrease in α-helical content of LC at the intermediate pH (*36*), and the LC structure significantly changes at pH 4.0 (*37*). Nearly identical CD spectra of intact and fragmented LC (Figure 6A) is not surprising, because in the three-dimensional structure of LC determined at 3.3 Å resolution for the whole BoNT/A neurotoxin (*35*, *38*) revealed that the cleavable bonds Y251−Y252 and F266-G267 are not contained in secondary structure (helix, sheet or turn).

Role of Zinc. Zinc, the natural cofactor of the LC, is bound at its active site. Catalytic activity of the preparation of LC employed in this study was inhibited by the presence of zinc in the assay mixture (see Results). Metalloproteases require metals to remain bound at the active sites to display protease activity, but are usually inhibited by excess metal in solution

(*29*). We reported earlier that catalytic activity of a zinc-free LC is restored by adding zinc to the assay mixture and the activity of a zinc-containing LC is inhibited by adding zinc to the reaction mixture (*1*). Similar results were also obtained with whole BoNT/A (*39*) and other metalloproteases (*29*). Moreover, a LC specific activity of 3.2 μmol min^{-1} mg^{-1} using the 17-mer SNAP-25 peptide substrate in the absence of exogenous zinc obtained in this study (see Results) is highest among all of LC preparations obtained thus far (*1*, *17*) or of the whole BoNT/A (*26*). Furthermore, the homogeneous nature of the LC preparation is supported by a single and sharp thermal transition of the LC at pH 6.5 (Figure 7). These considerations and our catalytic activity results led us to conclude that the LC preparation employed in this study was saturated with active-site zinc.

Adding zinc to this holo-LC preparations dramatically increased the rate of fragmentation (compare Figure 1, panel B with panel A). Thus, zinc must have a role other than an active-site catalytic role. Moreover, in a partially zinc-free LC preparation, adding $ZnCl_2$ failed to convert a IVA fragment to a IVB (see Figure 1) fragment (*17*) as found with the holo-LC preparation described here (compare Figure 1, panel B with panel A). Thus, zinc must have a structural or conformational role at or around the cleavable bonds in addition to its essential catalytic role. The midpoint of thermal transition, T_m of 41.5 °C at pH 6.5 (Figure 7), in the absence of added zinc, is comparable to 44 °C recently reported for LC at pH 7.5 and in the presence of NaCl (*27*), but is significantly lower than 52 °C determined for a hexa-His tagged LC in tris-HCl buffer pH 7.0 (*28*). These differences were most likely due to differences in the buffers employed and LC sequence. We cannot explain the apparent biphasic behavior of the thermal transition in the presence of $ZnCl_2$ (Figure 7). It is possible that excess zinc exerts more than one effect on the structure of LC, making it more thermostable than by low pH (T_m, 54 versus 50 °C). One stabilizing effect of zinc might relate to preferential binding of zinc to a second metal-binding site. Recently, Subramanyam Swaminathan detected and identified two additional divalent metal binding sites in the BoNT/B holotoxin structure by X-ray crystallography (personal communication). The first of these sites involves residues in the vicinity of the autocatalytic sites in BoNT/A LC. Interaction of excess zinc in solution with this second metal binding site might juxtapose the cleavable bonds to the active site. A second effect of zinc stabilizing a particular conformation that imparts additional thermostability to the LC may be that of a cosolvent. Natural ligands of proteins and cosubstrates of enzyme reactions are known to exert such effects on protein conformations. For example, stabilizing one of the several active conformations of tryptophan synthase is induced by solvent effects of monovalent cations (*40*) and of a cosubstrate, 2-mercaptoethanol (*41*).

Autocatalytic Cleavage Sites. Recently, we demonstrated that the LC undergoes C-terminal processing[2] at several sites between residues 419−448 and fragmentation[2] near the middle of the molecule, both by autocatalytic proteolysis (*17*). In that study, which employed a partially zinc-free LC, C-terminal processing was predominant, and fragmentation at the F266−G267 bond preceded the final cleavage (fragmentation at Y251−Y252) bond. In the presence of added $ZnCl_2$, fragmentation at Y251−Y252 occurred rapidly, bypassing cleavage at F266−G267, and was then followed by C-terminal processing. In the presence of the metal chelator, TPEN, or a competitive peptide inhibitor, CRATKML, fragmentation was prevented and C-terminal processing was drastically reduced. In the present study, which employed fully Zn-containing holo-LC, C-terminal processing (represented by appearance of IB in Figure 1A) was a minor event that did not lead to detectable cleavage at F266−G267 (absence of fragment IIIA). F266−G267 bond cleavage must therefore be related to loss of zinc from the protein's active site. Indeed, an active-site glutamic acid residue at position 261 in helix 4, only five residues preceding the F266−G267 bond at the end of the helix, forms part of the tetravalent coordination geometry of active-site zinc (*35*, *42*). Loss of zinc from the active site can make this region more flexible and susceptible to autocatalysis. Autocatalytic fragmentation at Y251−Y252 bond, at the tip of flexible loop C (*35*, *42*), is more pronounced and occurs in the partial zinc-depleted and in the fully zinc-containing LC. A recent preliminary report on the X-ray crystallographic studies of a C- and N-terminal truncated LC found the Y251−Y252 bond is cleaved at the active sites of a dimer (*34*).

Significance of the Autocatalytic Reaction. Significance of the fragmentation reaction of LC is intriguing. Autocatalytic proteolysis of expressed proteins has long been recognized as necessary events in generating highly active catalysts as in chymotrypsinogen−chymotrypsin (*43*) and pepsinogen−pepsin (*33*). Other consequences include triggering of apoptosis as in mammalian caspases (*21*) or in modifying an amino acid to generate a catalytic-site residue as in *S*-adenosyl methionine decarboxylase (*19*). In contrast, the situation with BoNT/A LC is quite different because autocatalysis does not enhance or abolish catalytic activity, nor is it known to be related to any cellular regulatory mechanism. The LC is naturally expressed by *Clostridia* as the N-terminal domain of a larger 150 kDa BoNT/A molecule. A posttranslational tryptic cleavage of the neurotoxin generates a dichain comprising the 50 kDa LC and the C-terminal 100 kDa domain still connected by a disulfide bond. The whole neurotoxin released by the bacterium is a complex with other protective proteins (*44*, *45*); the latter probably acts as a defensive tool for the bacteria, and there is no indication that the 150 kDa molecule undergoes autocatalysis (*16*), unlike the LC reported here. The 100 kDa chain is thought to contain a central, 50 kDa membrane translocation domain (H_n) and a C-terminal, 50 kDa domain (H_c) for binding the neurotoxins to specific receptors located exclusively on the peripheral cholinergic nerve endings (*8*). The H_n domain is believed to participate in a receptor-mediated endocytotic pore formation in an acidic environment, allowing translocation of the catalytic LC into the cytosol. Reducing the disulfide bond that connects the LC to H_n upon exposure to the cytosol or within the acidic endosome (*9*, *46*) is thought to expose the catalytic LC into the cytosol. Recent experiments using lipid bilayers clearly demonstrated that disulfide cleavage triggered translocation of LC alone through a HC channel at pH 5.0. Our experimental data on concentration dependence of rates at pH 5.0 (Figure 5B) suggest that if LC autocatalysis takes place within the acidic endosome, it can occur at a very low concentration, and fast enough during its few minutes of transit there (*36*). The in vitro cleavage half-life of 17 min determined at room

temperature (23 °C) in this study will be expected to be faster at a much higher physiological temperature of 37 °C. In addition, some unknown cellular factor could also enhance the reaction farther. Moreover, since the reaction is largely unimolecular at low pH, cleavage will not be retarded by the presence of other proteins (*47*). Experiments using cell lines to detect autocatalysis in vivo are in progress.

The BoNT/A activity against SNAP-25, its natural substrate, persists in cultured spinal cord cells for more than 11 weeks (*48*). This duration is much longer than employed in our experiments (0−14 days), which detected the fragmentation. In addition to pH, we found a variety of conditions such as buffer and salt composition and concentration, monovalent and divalent metal ions, as well as temperature and radiation that affect the fragmentation reaction (manuscript in preparation). Inside the cell, LC can thus be expected to be more susceptible to autocatalytic fragmentation. If autocatalysis indeed is also a phenomenon within intoxicated cells, what role or benefit does it add to the process of toxicity? The results presented in this paper clearly demonstrate that fragmentation of LC did not affect its catalytic activity at least in vitro. Although the prevalent hypothesis that cleavage of a specific bond in one of the SNARE proteins by the LC is due to BoNT toxicity leading to inhibition of neurotransmitter exocytosis, a second, nonproteolytic inhibitory mechanism involving activation of neuronal transglutaminase has also been proposed (*49*). Moreover, tyrosine phosphorylation of BoNT/A and BoNT/E by Src kinase has been reported to enhance both proteolytic activity and stability of the neurotoxins, and in case of at least the former, under in vivo conditions (*50*). It remains to be discovered if there is any correlation of the autocatalytic reaction described in this paper with the fate of LC, its phosphorylation or stability of BoNT/A proteolytic efficiency on SNAP-25 as well as any effect on transglutaminase activity inside the cells.

In conclusion, we demonstrated that autocatalytic fragmentation of BoNT/A LC did not lead to activation or inactivation of its zinc-endopeptidase catalytic activity. Autocatalysis is the result of both intramolecular and intermolecular reactions. Low pH and zinc appeared to stimulate the intramolecular reaction by several orders of magnitude, presumably by inducing a conformational change. Our findings suggest that the autocatalytic reaction is a possibility during translocation of BoNT/A LC through an acidic endosome.

ACKNOWLEDGMENT

We thank Ms. Kristi Fox and SPC Matthew Ludivico for the proteolysis experiments and enzyme assays, Dr. James J. Schmidt for a gift of the peptide inhibitor II, discussions, and critical reading of the manuscript, Mr. Wilson Ribot for use of the BioRad Gel scanner, and Drs. Frank Lebeda, Bal Ram Singh, and Major Charles B. Millard for valuable comments.

REFERENCES

1. Ahmed, S. A., and Smith, L. A. (2000) *J. Protein Chem. 19*, 475−87.
2. Montecucco, C., and Schiavo, G. (1995) *Q. Rev. Biophys. 28*, 423−72.
3. Schiavo, G., Shone, C. C., Bennett, M. K., Scheller, R. H., and Montecucco, C. (1995) *J. Biol. Chem. 270*, 10566−70.
4. Arnon, S. S., Schechter, R., Inglesby, T. V., Henderson, D. A., Bartlett, J. G., Ascher, M. S., Eitzen, E., Fine, A. D., Hauer, J., Layton, M., Lillibridge, S., Osterholm, M. T., O'Toole, T., Parker, G., Perl, T. M., Russell, P. K., Swerdlow, D. L., and Tonat, K. (2001) *JAMA 285*, 1059−70.
5. Steinhardt, R. A., Bi, G., and Alderton, J. M. (1994) *Science 263*, 390−3.
6. Verheyden, J., Blitzer, A., and Brin, M. F. (2001) *Semin. Cutaneous Med. Surg. 20*, 121−6.
7. Brin, M. F., Lew, M. F., Adler, C. H., Comella, C. L., Factor, S. A., Jankovic, J., O'Brien, C., Murray, J. J., Wallace, J. D., Willmer-Hulme, A., and Koller, M. (1999) *Neurology 53*, 1431−8.
8. Black, J. D., and Dolly, J. O. (1987) *Neuroscience 23*, 767−79.
9. Montal, M. S., Blewitt, R., Tomich, J. M., and Montal, M. (1992) *FEBS Lett. 313*, 12−8.
10. Grove, A., Iwamoto, T., Montal, M. S., Tomich, J. M., and Montal, M. (1992) *Methods Enzymol. 207*, 510−25.
11. Foran, P., Lawrence, G. W., Shone, C. C., Foster, K. A., and Dolly, J. O. (1996) *Biochemistry 35*, 2630−6.
12. Blasi, J., Chapman, E. R., Link, E., Binz, T., Yamasaki, S., De Camilli, P., Sudhof, T. C., Niemann, H., and Jahn, R. (1993) *Nature 365*, 160−3.
13. Schiavo, G., Rossetto, O., Catsicas, S., Polverino de Laureto, P., DasGupta, B. R., Benfenati, F., and Montecucco, C. (1993) *J. Biol. Chem. 268*, 23784−7.
14. Alderton, J. M., Ahmed, S. A., Smith, L. A., and Steinhardt, R. A. (2000) *Cell Calcium 28*, 161−9.
15. Zhou, L., de Paiva, A., Liu, D., Aoki, R., and Dolly, J. O. (1995) *Biochemistry 34*, 15175−81.
16. DasGupta, B. R., and Foley, J., Jr. (1989) *Biochimie 71*, 1193−200.
17. Ahmed, S. A., Byrne, M. P., Jensen, M., Hines, H. B., Brueggemann, E., and Smith, L. A. (2001) *J. Protein Chem. 20*, 221−31.
18. Kim, Y., Kim, S., Earnest, T. N., and Hol, W. G. (2002) *J. Biol. Chem. 277*, 2823−9.
19. Li, Y. F., Hess, S., Pannell, L. K., White Tabor, C., and Tabor, H. (2001) *Proc. Natl. Acad. Sci. U.S.A. 98*, 10578−83.
20. Strasser, A., O'Connor, L., and Dixit, V. M. (2000) *Annu. Rev. Biochem. 69*, 217−45.
21. Earnshaw, W. C., Martins, L. M., and Kaufmann, S. H. (1999) *Annu. Rev. Biochem. 68*, 383−424.
22. Schmidt, J. J., Stafford, R. G., and Bostian, K. A. (1998) *FEBS Lett. 435*, 61−4.
23. Schmidt, J. J., and Stafford, R. G. (2003) *FEBS Letter 69*, 297−303.
24. Laemmli, U. K. (1970) *Nature 227*, 680−5.
25. Schagger, H., and von Jagow, G. (1987) *Anal. Biochem. 166*, 368−79.
26. Schmidt, J. J., and Bostian, K. A. (1995) *J. Protein Chem. 14*, 703−8.
27. Binz, T., Bade, S., Rummel, A., Kollewe, A., and Alves, J. (2002) *Biochemistry 41*, 1717−23.
28. Li, L., and Singh, B. R. (2000) *Biochemistry 39*, 6466−74.
29. Auld, D. S. (1995) *Methods Enzymol. 248*, 228−42.
30. Voziyan, P. A., and Fisher, M. T. (2002) *Arch. Biochem. Biophys. 397*, 293−7.
31. Cai, S., and Singh, B. R. (2001) *Biochemistry 40*, 4693−702.
32. Ahmed, S. A., Martin, B., and Miles, E. W. (1986) *Biochemistry 25*, 4233−40.
33. McPhie, P. (1972) *J. Biol. Chem. 247*, 4277−81.
34. Knapp, M., Segelke, B., Balhorn, R., and Rupp, B. (2000) In *Abstract, 37th Annual Meeting of the Interagency Botulinum Research Coordinating Committee*, Alisomar, California.
35. Lacy, D. B., Tepp, W., Cohen, A. C., DasGupta, B. R., and Stevens, R. C. (1998) *Nat. Struct. Biol. 5*, 898−902.
36. Koriazova, L. K., and Montal, M. (2003) *Nat. Struct. Biol. 10*, 13−17.
37. Fu, F. N., Busath, D. D., and Singh, B. R. (2002) *Biophys. Chem. 99*, 17−29.
38. Lacy, D. B., and Stevens, R. C. (1999) *J. Mol. Biol. 291*, 1091−104.
39. Simpson, L. L., Maksymowych, A. B., and Hao, S. (2001) *J. Biol. Chem. 276*, 27034−41.
40. Ruvinov, S. B., Ahmed, S. A., McPhie, P., and Miles, E. W. (1995) *J. Biol. Chem. 270*, 17333−8.

41. Ahmed, S. A., McPhie, P., and Miles, E. W. (1996) *J. Biol. Chem. 271*, 29100−6.
42. Swaminathan, S., and Eswaramoorthy, S. (2000) *Nat. Struct. Biol. 7*, 693−9.
43. Stroud, R. M., Kossiakoff, A. A., and Chambers, J. L. (1977) *Annu. Rev. Biophys. Bioeng. 6*, 177−93.
44. Sharma, S. K., Fu, F. N., and Singh, B. R. (1999) *J. Protein Chem. 18*, 29−38.
45. Singh, B. R., Lopes, T., and Silvia, M. A. (1996) *Toxicon 34*, 267−75.
46. Oblatt-Montal, M., Yamazaki, M., Nelson, R., and Montal, M. (1995) *Protein Sci. 4*, 1490−7.
47. McPhie, P. (1974) *Biochem. Biophys. Res. Commun. 56*, 789−92.
48. Keller, J. E., Neale, E. A., Oyler, G., and Adler, M. (1999) *FEBS Lett. 456*, 137−42.
49. Deloye, F., Doussau, F., and Poulain, B. (1997) *C. R. Seances Soc. Biol. Ses. Fil. 191*, 433−50.
50. Ferrer-Montiel, A. V., Canaves, J. M., DasGupta, B. R., Wilson, M. C., and Montal, M. (1996) *J. Biol. Chem. 271*, 18322−5.
51. Singh, B. R., and DasGupta, B. R. (1989) *Mol. Cell Biochem. 85*, 67−73.

BI030062C